Korean J. Chem. Eng., **28**(6), 1474-1479 (2011)
DOI: 10.1007/s11814-010-0507-x

Computational fluid dynamics simulations of pressure drop and heat transfer in fixed bed reactor with spherical particles

Ali Reza Miroliaei, Farhad Shahraki†, and Hossein Atashi

Department of Chemical Engineering, University of Sistan and Baluchestan, Zahedan 98164-161, Iran
(*Received 8 August 2010 • accepted 3 December 2010*)

Abstract−Fixed bed reactors are among the most important equipment in chemical industries as these are used in chemical processes. An accurate insight into the fluid flow in these reactors is necessary for their modeling. The pressure drop and heat transfer coefficient have been studied for the fixed bed reactor with tube to particle diameter ratio (N) of 4.6 and comprising 130 spherical particles using computational fluid dynamics (CFD). The simulations were carried out in a wide range of Reynolds number: $3.85 \le Re \le 611.79$. The RNG k-ε turbulence model was used in the turbulent regime. The CFD results were compared with empirical correlations in the literature. The predicted pressure drop values in laminar flow were overestimated compared with the Ergun's [27] correlation and underestimated in the turbulent regime due to the wall friction and the flow channeling in the bed, respectively. It was observed that the CFD results of the pressure drop are in good agreement with the correlations of Zhavoronkov et al. [28] and Reichelt [29] because the wall effects have been taken into account in these correlations. Values of the predicted dimensionless heat transfer coefficient showed better agreement with the Dixon and Labua's [32] correlation. This is explained by the fact that this correlation is a function of the particle size and shape in the bed.

Key words: Fixed Bed Reactor, Pressure Drop, Heat Transfer Coefficient, Computational Fluid Dynamics, Turbulence Model

INTRODUCTION

Nowadays, more industrial catalytic processes in gas phase are carried out in fixed bed reactors. A fixed bed reactor includes stationary catalyst particles within a vertical tube. The chemical reactions are performed over the internal or external surface of catalyst into the bed [1]. Important industrial processes such as the Fischer-Tropsch synthesis process, steam reforming of methane, methanol synthesis process, ammonia synthesis process, and so on, have been carried out in fixed bed reactors [2]. Hot spot formation, high pressure drop and deactivation of the catalyst can cause improper performance of fixed bed reactors. Three designs, as shown in Fig. 1, for the optimal performance of fixed bed reactors have been suggested:

- Single bed units
- Multi bed units
- Multi tube units

The multi tube reactor is more common than the other two fixed bed designs because the heat transfer operation between the fluid and catalyst bed is better than the others' [1]. The energy and materials can be transferred with the proper distribution of fluid flow. The accurate motion of fluid will be acquired by controlling of pressure, gravity or surface forces or using rotating elements. Computational fluid dynamics (CFD) is a tool for achieving the mentioned purposes. The application of CFD has led to the optimum design of processes [3]. The study of fluid flow and heat transfer in a fixed bed reactor comprising 130 spherical particles and tube to particle diameter ratio N=4.6 has been carried out for both laminar and turbulent flow regimes at 3.85 Re 611.79.

†To whom correspondence should be addressed.
E-mail: fshahraki@eng.usb.ac.ir

BACKGROUND

The pressure drop is the most important parameter for design and validation of the accuracy of fluid flow in fixed bed reactors. This parameter has been studied experimentally by several researchers. The first experimental studies on pressure drop were carried out by Carman [4] and Coulson [5] in the creeping flow regime for the low N beds. They described the wall effects by including the surface area of the column in the definition of the drag coefficient. Eisfeld and Schnitzlein [6] studied the wall effects on pressure drop which were reported by Mehta and Hawley [7] and Foumeny et al. [8]. They reported that Ergun's equation gives good results in the creeping and turbulent flow regimes for N>10.

There are two methods for CFD simulation of fixed bed reactors. In the first approach, the bed is modeled using the pseudo-homogeneous approach. In this approach, the effective parameters are defined for dispersion and heat transfer and the radial profiles are constant along the axial direction of packed bed. This assumption may lead to errors in the study of transport phenomena in the fixed bed reactors. The velocity field can be obtained from a modified momentum balance. The continued lumping of transport phenomena is the disadvantage of this method.

In the second approach, the particles are placed separately in the bed. This method yields a detailed description of the fluid flow between the particles. The governing equations for the fluid flow are relatively simple, but the geometric modeling and grid generation become complicated. In this method, the contacts between particles together and particles to wall have been accounted [9].

Dalman et al. [10] performed CFD simulation of fluid flow and heat transfer around two spherical particles near the wall at Re< 200. Their simulations were carried out in 2D geometry. They showed

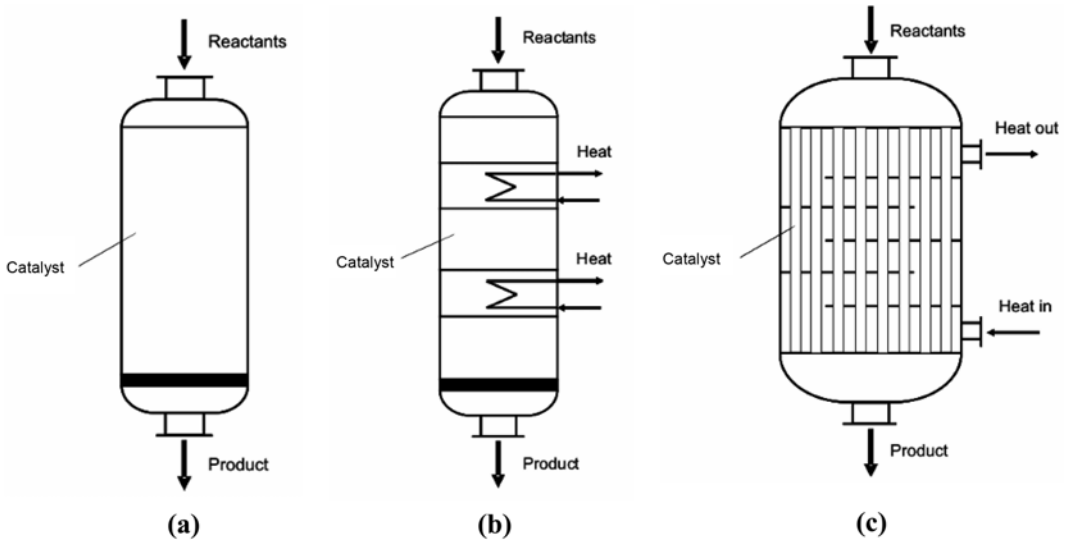

Fig. 1. Fixed bed reactors: (a) single bed units; (b) multi bed units; (c) multi tube units.

that eddies are formed between particles and lead to poor heat transfer regions. Lloyd and Boehm [11] studied the influence of the particles distance on the drag coefficient. They concluded that heat transfer from the particles decreases by decreasing particle distance. Derkx and Dixon [12] carried out 3D simulations in the fixed bed using finite element method for three spherical particles. The wall Nusselt number was reported for k-ε turbulence model at 25<Re<101. Calis et al. [13] simulated the pressure drop and drag coefficient in square channels in the range N between 1 and 2 by using CFX 5.3. The results showed good agreement with the LDA measurements. Nijemeisland and Dixon [14] compared the CFD results of fluid flow and heat transfer with the experimental results in the fixed bed of N=2 and having 44 particles. They used several correction factors for improvement of their simulations. The radiation effects were neglected in these simulations. Guardo et al. [15,16] investigated pressure drop and heat transfer in the fixed bed with N=3.923 in laminar and turbulent flow regimes. They found that CFD results of Spalart-Allmaras turbulence model agree better with the empirical correlations. Gunjal et al. [17] studied fluid flow through the array of spheres using the unit-cell approach. They studied the relative contributions of surface drag and form drag in overall resistance to the flow through packed bed reactors. The CFD and experimental results have been compared with different periodically repeating arrangements of particles. Dixon et al. [18] used CFD for study of wall conduction effect on the heat transfer in the fixed bed reactor tube with packings of spheres, full cylinders, and cylinders with internal voids. They concluded that the inclusion of wall conduction has no effect on the average wall temperature and redial temperature profiles in the bed, but the temperature distribution on the wall changes considerably. Wen and Ding [19] studied heat transfer behavior in packed bed. In their study, effective thermal conductivities and convective heat transfer coefficient have been reported under the constant wall temperature conditions. Their results have shown that a large temperature drop occurs at the wall region and two-dimensional axial dispersion plug flow (2DADPF) model can predict the axial temperature distribution fairly well, but the prediction is poor for the radial temperature distribution. Reddy and Joshi [20] calculated pressure drop and drag coefficients in the fixed and the expanded beds. The CFD results have been compared with Ergun's equation in laminar and turbulent flow regimes. Their results showed good agreement with the findings of Mehta and Hawley, Foumeny et al. and Eisfeld and Schnitzlein. Atmakidis and Kenig [21] investigated the wall effect on pressure drop in the laminar flow regime in moderate N. They compared their CFD results with experimental pressure drop correlations where the results were in good agreement with the correlations of Zhavoronkov et al. and Reichelt. Reddy and Joshi [22] investigated wall effects in three fixed beds with N= 3, 5, 10 in the creeping, transition and turbulent flow regimes. They concluded that the effects of wall friction and flow channeling decrease as N increases in the creeping and turbulent flow regimes.

1. Fluid Flow Regimes in the Fixed Bed Reactors

There are several methods for visualization of flow regimes in porous media. LDA, MRI and PIV are the most important methods. LDA and PIV can be used only in solid and liquid phases of the same refractive index, whereas MRI requires that the porous media be nonmagnetic. So far, the MRI method has been used at low flow rates in high N beds [13,23].

The fluid flow regimes in the fixed bed reactors depend on the physical properties of fluid such as density and viscosity, compressibility; size, shape and roughness of the particles, tube to particle diameter ratio; the kinematic variables such as the flow rates, pressure and temperature; as well as the mechanical characteristics such as the design of distributors, etc. Four flow regimes proposed by Dybbs and Edwards [24] in the fixed bed reactors that were reviewed by Dixon et al. [25] are as follows:

1. The Darcy or creeping flow regime at Re_i<1: Pressure drop is linearly proportional to interstitial flow rate and flow is dominated by viscous forces.

2. A steady laminar flow regime at 10<Re_i<150: Pressure drop has nonlinear relationship with interstitial flow rate.

3. An unsteady laminar flow regime at 150<Re_i<300: Laminar wake oscillations appear in the pores and vortices form at around Re_i=250.

4. A highly unsteady flow regime at Re_i>300: Eddies formed

are similar to turbulent flow in pipes.

CFD MODELING

1. Governing Equations

The CFD methods use numerical techniques for solving the governing equations in the fluid flow such as continuity, momentum and energy equations. In the absence of a chemical reaction, the fluid flow field and heat transfer can be determined by solving the following equations:

1-1. Continuity Equation

The general form of the continuity equation can be expressed as follows:

$$\frac{\partial \rho}{\partial t}+\frac{\partial(\rho u_i)}{\partial x_i}=S_m \tag{1}$$

In this equation S_m is the mass added through phase changes or user defined sources.

1-2. Momentum Equation

Navier-Stokes equations have been used for description of momentum equations. The equation for conservation of momentum in the *i*-direction is defined by:

$$\frac{\partial(\rho u_i)}{\partial t}+\frac{\partial(\rho u_i u_j)}{\partial x_j}=-\frac{\partial P}{\partial x_i}+\frac{\partial \tau_{ij}}{\partial x_j}+\rho g_i+F_i \tag{2}$$

ρg_i and F_i are the gravitational body force and a external body forces component, respectively.

1-3. Energy Equation

The energy equation is solved in the form of a transport equation for static temperature. The temperature equation is obtained from the enthalpy equation, by taking the temperature as a dependent variable. The enthalpy equation is defined as:

$$\frac{\partial(\rho h)}{\partial t}+\frac{\partial(\rho u_i h)}{\partial x_i}=\frac{\partial}{\partial x_i}(\lambda+\lambda_t)\frac{\partial T}{\partial x_i} - \frac{\partial \sum_j h_j J_j}{\partial x_i}+\frac{DP}{Dt}+(\tau_{ik})_{eff}\frac{\partial u_i}{\partial x_k}+S_h \tag{3}$$

S_h includes heat of chemical reaction, any interphase exchange of heat, and any other user-defined volumetric heat sources. S_m, F_i and S_h are equal to zero in our simulations.

2. Geometry and Boundary Conditions

The 3-D geometry comprising 130 spherical particles with 5 mm diameter was used in CFD simulations. The geometry and unstructured tetrahedral mesh were generated by using commercial software GAMBIT 2.0.4. In the present work, the continuity, momentum and energy equations were solved with commercial CFD package, ANSYS FLUENT 12.0.16. The boundary conditions used at steady-state flow are as follows:

1. constant temperature and velocity at the inlet;
2. constant temperature at the wall (473.15 K);
3. constant pressure at the outlet (1 atm);
4. no-slip velocity condition at the wall and particle surfaces.

Air was chosen for fluid flow and heat transfer simulations in the fixed bed. The incompressible ideal gas law and the power law were used for dependency of density and viscosity on the temperature, respectively. The pressure-velocity coupling was carried out by the SIMPLE scheme. Second-order upwind schemes were used for the convective terms in the momentum, energy and turbulence equations to achieve more accuracy in the results.

RESULTS AND DISCUSSION

The CFD results of pressure drop and heat transfer coefficient were compared with empirical correlations in a wide range of Reynolds number from 3.85 to 611.79. The RNG k-ε turbulence model was used in turbulent regime. This model has an additional term in its equation that the flow features such as strong streamline curvature, vortices, and rotation take into account. These features make the RNG k-ε model more suitable for complex flows, such as flow in fixed beds [26].

1. Pressure Drop in the Fixed Bed

The correlations proposed by Ergun [27], Zhavoronkov et al. [28] and Reichelt [29] have been selected for validation of CFD results. The wall effects have been taken into account in Zhavoronkov et al. and Reichelt's equations.

The following semi-empirical correlation for laminar and turbulent flows has been suggested by Ergun [27]:

$$\frac{\Delta P}{L}=150\frac{\mu u}{d_P^2\varphi^2}\frac{(1-\varepsilon)^2}{\varepsilon^3}+1.75\frac{\rho u^2}{d_P\varphi}\frac{(1-\varepsilon)}{\varepsilon^3} \tag{4}$$

Zhavoronkov et al. [28] presented the following correlation in a wide range of Reynolds number:

$$\frac{\Delta P}{L}=A\frac{\mu u(1-\varepsilon)^2}{d_p^2}\frac{}{\varepsilon^3}+B\frac{\rho u^2}{d_p}\frac{(1-\varepsilon)}{\varepsilon^3} \tag{5}$$

In this equation the wall effects have been taken into account in parameters A and B as follows:

$$A=163.35A_w^2 \tag{6a}$$

$$B=1.2B_w \tag{6b}$$

$$A_w=B_w=1+\frac{1}{2(D/d_p)(1-\varepsilon)} \tag{6c}$$

The correction of Ergun's equation has been performed by Reichelt [29] as follows:

$$\frac{\Delta P}{L}=K_1A_w^2\frac{\mu u(1-\varepsilon)^2}{d_p^2}\frac{}{\varepsilon^3}+\frac{A_w\rho u^2}{B_w\ d_p}\frac{(1-\varepsilon)}{\varepsilon^3} \tag{7}$$

where

$$A_w=1+\frac{2}{3(D/d_p)(1-\varepsilon)} \tag{8a}$$

$$B_w=[k_1(d_p/D)^2+k_2]^2 \tag{8b}$$

In Eqs. (7) and (8b), K_1, k_1 and k_2 are equal 154, 1.15 and 0.87 for spherical particles in the bed, respectively.

The CFD results are compared with the correlations of Ergun, Zhavoronkov et al. and Reichelt in the laminar and turbulent flow regimes as shown in Fig. 2. It can be seen that the results obtained from the CFD simulations agree with those estimated using experimental data. Interestingly, in comparison with Ergun's equation, the simulated pressure drop values are overestimated in the range

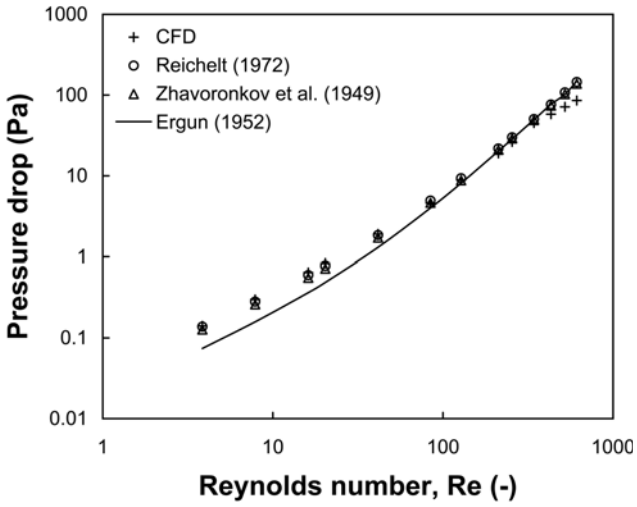

Fig. 2. Pressure drop vs. Reynolds number.

of Re<150 due to wall friction or viscose forces effects in the wall and underestimated in the range of Re>150 due to flow channeling in the bed. As mentioned before, the predicted pressure drop values agree better with the correlations of Zhavoronkov et al. and Reichelt than the Ergun's correlation because the wall effects on pressure drop have been taken into account in these correlations.

2. Velocity Vectors Profile

In Fig. 3, velocity vectors are shown for three Re values: Re= 3.85, 127.84 and 611.79. The length of an arrow is proportional to the magnitude of the velocity vector, and the arrow points in the same direction as the local flow. In Fig. 3(a), local velocities in the bed are approximately equal to superficial velocity, but local velocities in the bed are approximately 10 and 3 times higher than the superficial velocity in Figs. 3(b) and 3(c), respectively. Near the wall and in the contact points, fluid flow is less than other points in the bed. In the interstices between particles, fluid flow is faster than the

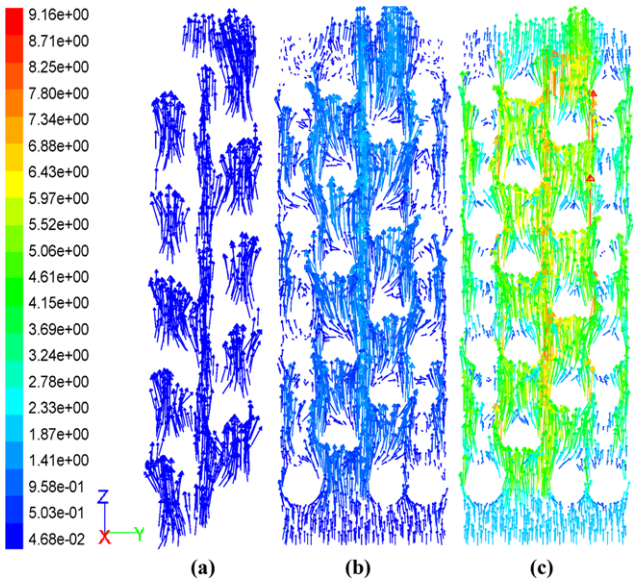

Fig. 3. Velocity vectors profile at (a) Re=3.85; (b) Re=127.84; (c) Re=611.79; legend shows velocity (m s^{-1}).

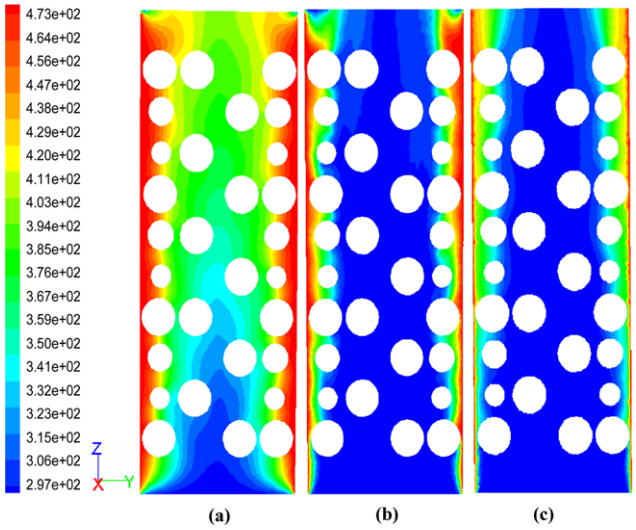

Fig. 4. Temperature contours at (a) Re=3.85; (b) Re=127.84; (c) Re=611.79; legend shows temperature (K).

other regions. It is observed that flow channeling takes place in the bed and increases with increasing the flow rate.

3. Temperature Contours in the Fixed Bed

The temperature contours in the bed are shown in Fig. 4 for three mentioned Re values. The heat diffusion into the bed causes the development of thermal boundary layer near the wall. At low flow rates, heat diffusion is too much from the wall into the bed. As Re increases, the difference between the wall and fluid temperatures increases and thickness of thermal boundary layer decreases. Consequently, the same distribution of temperature obtains in the bed.

4. Heat Transfer Coefficient

The heat transfer model is validated by comparison of CFD and empirical results. Several correlations for the calculation of heat transfer coefficient in the fixed bed reactors can be found in the literature. For example, Yagi and Wakao [30] expressed the following correlations:

$$Nu_{wf}=\begin{cases}0.6Pr^{1/3}Re^{1/2} & 1\le Re\le 40\\ 0.2Pr^{1/3}Re^{0.8} & 40\le Re\le 2000\end{cases} \quad (9)$$

The validity of the correlation of Yagi and Wakao for low values of Re is in some doubt owing to the neglect of axial dispersion in the analysis of the data.

The correlation proposed by Li and Finlayson [31] for 3.3≤N≤ 20 is expressed as follows:

$$Nu_{wf}=0.17Re^{0.79} \qquad 20\le Re\le 7600 \quad (10)$$

This correlation is not dependent on the tube to particle diameter ratio.

Dixon and Labua [32] entered the effect of tube to particle diameter ratio in their correlation as follows:

$$Nu_{wf}=\left(1-\frac{1}{N}\right)Pr^{1/3}Re^{0.61} \qquad Re>100 \quad (11)$$

Demirel et al. [33] proposed the following correlation for 4.5≤N≤7.5:

$$Nu_{wf}=0.217Re^{0.756} \qquad 200\le Re\le 1450 \quad (12)$$

The comparison between CFD and empirical results for dimension-

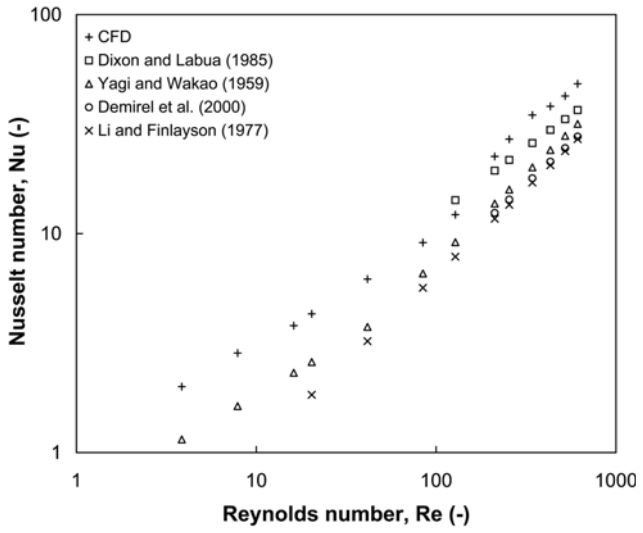

Fig. 5. Nusselt number vs. Reynolds number.

less heat transfer coefficient versus Reynolds number is shown in Fig. 5. From Fig. 5, the precision of CFD results is poor compared with the correlations of Li and Finlayson and Demirel et al. As mentioned earlier, the CFD results have too much difference with the Yagi and Wakao's correlations in the low Re numbers, but the predictions are fairly good in the turbulent flow regime. It can be seen that CFD results are in good agreement with Dixon and Labua's correlation because the effects of the particles size and shape in the bed have been taken into account in this correlation.

CONCLUSION

The pressure drop and heat transfer coefficient were simulated in a fixed bed reactor with N=4.6 and comprising 130 spherical particles in laminar and turbulent flow regimes. In general, the pressure drop depends on the velocity field. For N<10, increasing the wall effects and void fraction near the wall has a high impact on total pressure drop in the bed. The simulated pressure drop values were compared with the empirical correlations of Ergun [27], Zhavoronkov et al. [28] and Reichelt [29]. The CFD results showed better agreement with the correlation of Zhavoronkov et al. and Reichelt in comparison with Ergun's equation, since wall effects have been taken into account in these correlations. As mentioned, for the reason wall effects in low Reynolds number, the pressure drop was overestimated as compared with Ergun's equation and underestimated in high Reynolds number because flow channeling takes place in the bed. The heat transfer coefficient was compared with several empirical correlations in the literature [30-33]. The CFD results were in a good agreement with the results of Dixon and Labua [32]. These results became better when the RNG k-ε turbulence model was used in high flow rates. In general, we can use the CFD simulation results with a high degree of confidence to design fixed bed reactors.

NOMENCLATURE

A, B, A_w, B_w : coefficients in Eqs. (5), (6), (7) and (8) [-]
D : tube diameter [m]
d_p : particle diameter [m]
ΔP : pressure drop [Pa]
F_i : external body forces component in direction i [N m^{-3}]
g_i : gravity acceleration in direction i [m s^{-2}]
h_i : fluid enthalpy of species i [kJ kg^{-1}]
J_j : diffusion flux of species i [kg m^{-2} s^{-1}]
L : height of bed or length of tube [m]
P : static pressure [Pa]
S_h : volumetric heat source [J m^{-3} s^{-1}]
S_m : volumetric mass source [kg m^{-3} s^{-1}]
T : temperature [K]
t : time [s]
u : superficial velocity [m s^{-1}]
x : coordinate [m]

Greek Letters

ε : bed porosity [-]
λ : thermal conductivity of fluid [W m^{-1} K^{-1}]
λ_t : turbulent thermal conductivity [W m^{-1} K^{-1}]
μ : molecular viscosity [Pa s]
ρ : density [kg m^{-3}]
φ : shape factor [-]
τ : deviatoric stress tensor [Pa]

Dimensionless Numbers

Nu=(hd_p/λ) : particle Nusselt number
Pr=($c_p\mu/\lambda$) : prandtl number
Re=($\rho ud_p/\mu$) : superficial Reynolds number
Re_i=($\rho ud_p/\mu\varepsilon$) : interstitial Reynolds number

Abbreviations

CFD : computational fluid dynamics
LDA : laser doppler anemometer
MRI : magnetic resonance imaging
PIV : particle image velocimetry
RNG : renormalized group
SIMPLE : semi implicit method for pressure linked equations

REFERENCES

1. H. A. Jakobsen, *Chemical reactor modeling multiphase reactive flows*, Springer-Verlag, Berlin Heidelberg, 954 (2008).
2. V. V. Ranade, *Computational flow modeling for chemical reactor engineering*, Academic Press, New York, 403 (2002).
3. J. B. Joshi and V. V. Ranade, *Ind. Eng. Chem. Res*., **42**, 1115 (2003).
4. P. C. Carman, *Trans. Inst. Chem. Eng.*, **15**, 150 (1937).
5. J. M. Coulson, *Trans. Inst. Chem. Eng.*, **27**, 237 (1949).
6. B. Eisfeld and K. Schnitzlein, *Chem. Eng. Sci*., **56**, 4321 (2001).
7. D. Mehta and M. C. Hawley, *Ind. Eng. Chem*., **8**, 280 (1969).
8. E. A. Foumeny, F. Benyahia, J. A. A. Castro, H. A. Moallemi and S. Roshani, *Int. J. Heat Mass Transfer*, **36**, 536 (1993).
9. M. Nijemeisland and A. G. Dixon, *AIChE J*., **50**, 906 (2004).
10. M. T. Dalman, J. H. Merkin and C. McGreavy, *Computers and Fluids*, **14**, 267 (1986).
11. B. Lloyd and R. Boehm, *Numer. Heat Trans. A*, **26**, 237 (1994).
12. O. R. Derkx and A. G. Dixon, *Numer. Heat Trans. A*, **29**, 777 (1996).
13. H. P. A. Calis, J. Nijenhuis, B. C. Paikert, F. M. Dautzenberg and

C. M. van den Bleek, *Chem. Eng. Sci*., **56**, 1713 (2001).
14. M. Nijemeisland and A. G. Dixon, *Chem. Eng. J*., **82**, 231 (2001).
15. A. Guardo, M. Coussirat, M. A. Larrayoz, F. Recasens and E. Egusquiza, *Ind. Eng. Chem. Res*., **43**, 7049 (2004).
16. A. Guardo, M. Coussirat, M. A. Larrayoz, F. Recasens and E. Egusquiza, *Chem. Eng. Sci*., **60**, 1733 (2005).
17. P. R. Gunjal, V. V. Ranade and R. V. Chaudhari, *AIChE J*., **51**, 365 (2005).
18. A. G. Dixon, M. Nijemeisland and E. H. Stitt, *Ind. Eng. Chem. Res*., **44**, 6342 (2005).
19. D. Wen and Y. Ding, *Chem. Eng. Sci*., **61**, 3532 (2006).
20. R. K. Reddy and J. B. Joshi, *Chem. Eng. Res. Des*., **86**, 444 (2008).
21. T. Atmakidis and E. Y. Kenig, *Chem. Eng. J*., **155**, 404 (2009).
22. R. K. Reddy and J. B. Joshi, *Particuology*, **8**, 37 (2010).
23. T. Suekane, Y. Yokouchi and Sh. Hirai, *AIChE J*., **49**, 10 (2003).
24. A. Dybbs and R. V. Edwards, *fundamentals of transport phenomena in porous media*, J. Bear and M. Corapcioglu, Eds., Martinus Nijhoff, Dordrecht, 201 (1984).
25. A. G. Dixon, M. Nijemeisland and E. H. Stitt, *Adv. Chem. Eng*., **31**, 307 (2006).
26. ANSYS FLUENT 12.0, User's Guide, 12.6.2 Modeling Turbulence, ANSYS, Inc. (2009).
27. S. Ergun, *Chem. Eng. Prog*., **48**, 89 (1952).
28. N. M. Zhavoronkov, M. E. Aerov and N. N. Umnik, *J. Phys. Chem*., **23**, 342 (1949).
29. W. Reichelt, *Chem. Ing. Tech*., **44**, 1068 (1972).
30. S. Yagi and N. Wakao, *AIChE J*., **5**, 79 (1959).
31. C. H. Li and B. A. Finlayson, *Chem. Eng. Sci*., **32**, 1055 (1977).
32. A. G. Dixon and L. A. LaBua, *Int. J. Heat Mass Transfer*, **28**, 879 (1985).
33. Y. Demirel, R. N. Sharma and H. H. Al-Ali, *Int. J. Heat Mass Transfer*, **43**, 327 (2000).